Proceedings of *RAGtime 23–25*
Z. Stuchlík, G. Török, V. Karas and D. Lančová, editors, Silesian University in Opava, 2023, pp. 83–91

Collapsing massive stars with self-gravity and their electromagnetic transients

Agnieszka Janiuk,[1,a] Narjes Shahamat[2] and Dominika Król[3]

[1]Center for Theoretical Physics, Polish Academy of Sciences
Al. Lotników 32/46, 02-668, Warsaw, Poland
[2]Department of Physics, School of Science
Ferdowsi University, Mashhad, Iran
[3]Astronomical Observatory, Jagiellonian University
Kraków, Poland
[a]agnes@cft.edu.pl

ABSTRACT
We investigate the fate of a collapsing stellar core, which is the final state of evolution of a massive, rotating star of a Wolf-Rayet type. Such stars explode as type I b/c supernovae, which have been observed in association with long gamma-ray bursts (GRBs). The core of the star is potentially forming a black hole, which is embedded in a dense, rotating, and possibly highly magnetized envelope. We study the process of collapse using General Relativistic MHD simulations, and we account for the growth of the black hole mass and its spin, as well as the related evolution of the spacetime metric. We find that some particular configurations of the initial black hole spin, the content of angular momentum in the stellar core, and the magnetic field configuration and its strength are favoured for producing a bright electromagnetic transient (i.e., a gamma-ray burst). On the other hand, most of the typical configurations studied in our models do not lead to a transient electromagnetic explosion and will end up in a direct collapse, accompanied by some residual variability induced by changing accretion rate. We also study the role of self-gravity in the stellar core and quantify the relative strength of the interfacial instabilities, such as Self-Gravity Interfacial (SGI) instability and Rayleigh-Taylor (RT), which may account for the production of an inhomogeneous structure, including spikes and bubbles, through the inner radii of the collapsing core (inside $\sim 200\, r_g$). We find that in self-gravitating collapsars, the RT modes cannot grow efficiently. We also conclude that transonic shocks are formed in the collapsing envelope, but they are weaker in magnetized stars.

Keywords: Accretion–black hole physics – gravitation – magnetohydrodynamics – massive stars – gamma-ray bursts

1 INTRODUCTION

Long gamma-ray bursts (GRBs) originate from the collapse of massive, rotating stars. Some of the GRBs exhibit much stronger variability patterns in the prompt GRB emis-

978-80-7510-577-6

sion than the usual stochastic variations. We discuss the mechanisms of these variations in the frame of the self-gravitating collapsar model.

Our computations confirm that gravitational instability can account for flaring activity in GRBs and the variations in their prompt emission. Rapid variability detected in the brightest GRBs, most likely powered by spinning black holes, is consistent with the self-gravitating collapsar model, where the density inhomogeneities are formed. The transonic shocks may also appear, but their effect should be weakened by the magnetic field.

We calculate the time evolution of the collapsing massive star using the General Relativistic Magneto-Hydrodynamic (GR MHD) scheme. We have developed a new version of the code HARM-METRIC, upgraded from that presented in Janiuk et al. (2018). The evolution of the space-time Kerr metric is accounted for by the increasing mass and changing spin of the black hole. We also added new terms that describe the self-gravity of the star and are changing at every time step during dynamical simulation.

In our formulation, the black hole has already been formed in the centre of the collapsing stellar core and its initial mass in of $3M_\odot$. Our computational grid size is 1000 r_g, which makes it smaller than a compact C-O core of a Wolf-Rayet star or a presupernova. Therefore, our model is compact enough to address the problem of self-gravitating gas close to the horizon of a newly formed black hole, but we do not address any prior or ongoing supernova explosion.

Depending on the rotation of the star, the ultimate outcome might be either a direct collapse or the formation of a mini-disc inside the core, that is, a collapsar which may lead to an electromagnetic transient. At the onset of the GRB, the collapsar consists of a black hole, a stellar envelope composed of accreting shells with decreasing density, and a rotationally supported disc formed at the equatorial region. At any chosen radius above the horizon, the gas is subject to gravity force induced by the Kerr black hole, the centrifugal force due to envelope rotation, and in addition, it feels the perturbative force due to the self-gravity of the matter enclosed within a given radius.

2 NUMERICAL CODE AND SETUP

We use the general relativistic MHD code called high-accuracy relativistic magnetohydrodynamics (HARM), originally published by Gammie et al. (2003) and further developed by various groups. Our code version, HARM-METRIC, includes the Kerr metric evolution, as first described in Janiuk et al. (2018).

The code introduces a conservative, shock-capturing scheme with low numerical viscosity to solve the hyperbolic system of partial differential equations of GR MHD. The numerical scheme uses the plasma energy-momentum tensor, with contributions from matter (gas) and electromagnetic field. For the GR MHD evolution, two fundamental equations are solved for the mass and energy-momentum conservation

$$(\rho u^\mu)_{;\mu} = 0, \qquad T^\mu_{\nu;\mu} = 0, \tag{1}$$

$$T^{\mu\nu}_{(m)} = \rho h u^\mu u^\nu + p g^{\mu\nu}, \tag{2}$$

Physical quantity	Geometrical units	cgs units
Length	$r_g = \frac{GM}{c^2}$	4.44×10^5 cm
Time	$T_{unit} = \frac{r_g}{c}$	1.38×10^{-5} s

Table 1. Conversion units between numerical code and physical scale of the collapsar.

$$T^{\mu\nu}_{(em)} = b^k b_k h u^\mu u^\nu + \frac{1}{2} b^k b_k g^{\mu\nu} - b^\mu b^\nu, \tag{3}$$

$$T^{\mu\nu} = T^{\mu\nu}_{(m)} + T^{\mu\nu}_{(em)}. \tag{4}$$

An additional constraint is given by the Equation of State (EOS). In the current project, we used an analytic form of adiabatic EOS that relates gas pressure with density. This scale, with a power of 4/3, is adequate for a relativistic gas of degenerate particles

$$p = K\rho^\gamma, \qquad \gamma = \frac{4}{3}. \tag{5}$$

The HARM code works in dimensionless units of G = c = 1. Conversion coefficients can be found in 1, where the black hole of 3 Solar masses is assumed. Notice that in the plots below, we use geometric units to express distance, while physical units are used to express time.

2.1 Initial conditions

Initial conditions for our collapsing stellar core are given by the quasi-spherical distribution of gas endowed with small angular momentum, concentrated at the equatorial plane (Król and Janiuk, 2021). The distributions of density and radial velocity are obtained from the Bondi solution, integrated numerically below and above the sonic point. The sonic point is a parameter of our model, and here it is assumed at $80 r_g$. Below this point, matter flows into a black hole supersonically and reaches the speed of light at the horizon.

We illustrate the initial condition in Figure 1, left panel. The density of the gas is normalised to physical units (given in cgs on the plot), assuming that the collapsing star has the initial mass of 25 Solar masses. This mass is enclosed within our computational domain with an outer radius of a $R_{\rm out} = 1000 r_g$. The plot shows only the innermost region of 100 r_g. Most mass of the core is located very near to the center, as it represents the evolved state of stellar evolution with a compact (iron) core formed.

In the initial conditions, we also introduce a small angular momentum imposed on the spherically distributed gas. The specific angular momentum is normalised by the parameter

S, with respect to that at the innermost stable circular orbit (ISCO). In addition, the rotation velocity scales with the polar angle to be maximal at the equator, $\theta = \pi/2$.

$$l = S\, l_{\rm isco} r^2 \sin^2\theta, \tag{6}$$

with

$$l_{\rm isco} = u_{\phi,{\rm isco}} = \frac{r_{\rm isco}^{1/2} - 2a/r_{\rm isco} + a^2/r_{\rm isco}^{3/2}}{\sqrt{1 - 3/r_{\rm isco} + 2a/r_{\rm isco}^{3/2}}}. \tag{7}$$

Notice that the radius $r_{\rm ISCO}$ in Kerr geometry depends on the black hole spin. In this proceeding, we show results obtained for the value of initial black hole spin $a_0 = 0.5$. We use several values of rotation parameter, as denoted on the plots in the next sections.

After the onset of collapse, the rotation of gas induces the formation of a mini-disk, i.e. toroidal structure, located at the equatorial plane. The density distribution becomes no longer spherical. Also, the radial velocity is decreased as the gas is subject to a centrifugal barrier. Flow is falling into the black hole with supersonic speed from the poles, while at the equator, the speed is subsonic.

The map on Figure 1, right panel, shows the flow distribution at time t=0.089 s for the model normalized with rotation parameter S=1.4. This means that the specific angular momentum is above a critical value (S=1), which allows for the formation of a rotationally supported torus. The sonic surface, Mach=1, is plotted with a solid line and marks the location of a transonic shock at the equatorial region.

3 IMPACT OF SELF-GRAVITY ON THE COLLAPSE

In our new simulations, both the mass and angular momentum accreted onto the event horizon – and used to update the Kerr metric coefficients – are now modified by the perturbation acting on the metric in the region above the horizon due to the self-gravity force that the gas feels at a given distance from the horizon. These perturbative terms are calculated from the stress-energy tensor. Therefore, in addition to the two equations governing the growth of black hole mass and spin via the mass and angular momentum transfer through the horizon, as given below, (Król and Janiuk, 2021), we now add perturbative terms to mass and angular momentum, computed at every radius above the event horizon.

$$\dot{M}_{\rm BH} = \int {\rm d}\theta{\rm d}\phi\ \sqrt{-g}\, T^r{}_t, \tag{8}$$

$$\dot{J} = \int {\rm d}\theta{\rm d}\phi\ \sqrt{-g}\, T^r{}_\phi, \tag{9}$$

$$\delta M_{\rm BH}(t,r) = 2\pi \int_{r_{\rm hor}}^{r} T^r_t\, \sqrt{-g}{\rm d}\theta, \tag{10}$$

$$\delta J(t,r) = 2\pi \int_{r_{\rm hor}}^{r} T^{r}_{\phi} \sqrt{-g} \mathrm{d}\theta, \tag{11}$$

$$\delta a = \frac{J + \delta J(r)}{M_{\rm BH} + \delta M_{\rm BH}(r)} - a^{i}, \tag{12}$$

$$a^{i} = a^{i-1} + \Delta a. \tag{13}$$

The terms computed in addition to mass and angular momentum changes (Janiuk et al., 2018) as these self-gravity perturbations are integrated at each grid point in the radial direction and at each time. They affect the change of Kerr metric coefficients, which are sensitive to the mass and spin updates. The dimensionless black hole spin, a, evolves as a result of black hole mass and angular momentum changes due to the accretion of mass under the horizon and is additionally changed due to the self-gravity of the collapsing core. The numerical method has been described in detail in Janiuk et al. (2023). Below, we compare the results of self-gravitating collapsar models to the runs without self-gravity in order to emphasize the difference and to investigate the role of self-gravity in collapsar physics.

As shown in Figure 2, the results are strongly sensitive to the adopted self-gravity effects and also weakly sensitive to the rotation of the collapsing envelope. The latter is normalized with respect to the critical angular momentum, for which the flow is circularized at the innermost stable orbit, ISCO (Król and Janiuk, 2021). In addition, the rotation velocity scales with the polar angle so that at the equator, the rotation of the star is maximal. We notice that the larger the initial rotation magnitude, the longer it takes for the black hole mass to evolve. The non-SG simulations end with very different final black hole mass, depending on the rotation parameter.

In contrast, the self-gravity of the envelope can speed up the evolution of the collapsing stellar core significantly. Also, the accretion rate and its fluctuations are of much higher amplitude when self-gravity effects are taken into account. Without self-gravity, there are longer time intervals where there is considerably less fluctuation of the accretion rate; in this case, there exist only some small oscillations in the accretion rate during some time intervals (around 0.2 s for S=1.4, and 0.4-0.5 s for S=2).

3.1 Instabilities on the collapsing core

As an effect of self-gravity, we observe density inhomogeneities and formation of the accretion shocks in all our models, regardless of the initial black hole spin or rotation parameter of the collapsar. First, there appears an equatorial outflow of matter, which reaches radii of up to about 80 $r_{\rm g}$ and is then stalled in the transonic shock. The small inhomogeneities in the pressure and density at the chosen time intervals are visible in more detail in the plots below, in Figure 3 and in Figure 4, respectively.

We quantify the inhomogeneities in the collapsar by computing the radial derivatives of density and pressure at specific times and locations. We identify the mechanism for

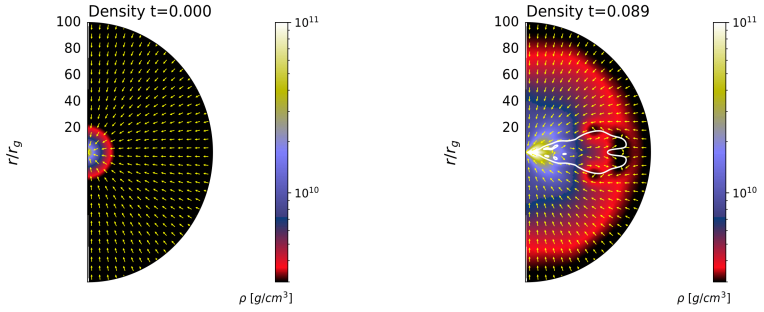

Figure 1. Left: Density distribution at the onset of core collapse. Arrows represent the velocity field (normalised length). Density distribution and velocity field after the onset of collapse. The model is parameterized with rotation parameter S=1.4. The thick white line represents the sonic surface, Mach=1. **Right:** Density distribution at the onset of core collapse. Arrows represent the velocity field.

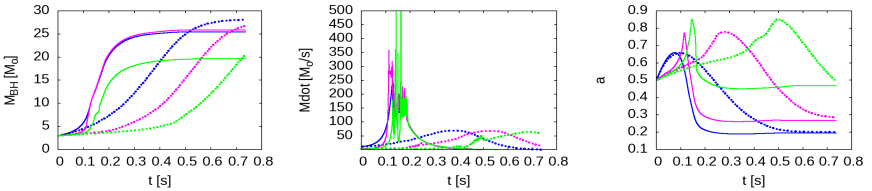

Figure 2. Left: Black hole mass changing as a function of time during the collapse. We start from 3 Solar mass black hole. Models including and excluding self-gravity are plotted by the thick and thin curves, respectively. Three colors refer to different amounts of angular momentum in the collapsing star: S=1.0 (blue), S=1.4 (red) and S=2.0 (green). **Middle:** Evolution of accretion rate through the horizon for self-gravitating and non-self-gravitating collapsars, shown with thick and thin lines, respectively. The different colors refer to various amounts of angular momentum in the collapsar, the same as in the left plot. **Right:** Evolution of the black hole dimensionless spin parameter during the collapse. We start from an oderately spinning black hole with a=0.5. Models including and excluding self-gravity are plotted by the thick and thin curves, respectively. Three color refer to different amounts of angular momentum in the collapsing star, the same as in the left and middle plots.

their creation as the SGI instability (Self-Gravity Interfacial instability), and we compare its strength with another well-known hydrodynamical instability, the Rayleigh-Taylor (RT) instability. Their growth rates are given as below (Kifonidis et al., 2003; Hunter Jr et al., 1997)

$$\sigma_{\rm RT} = \sqrt{-\frac{p}{\rho}\frac{\partial ln\rho}{\partial r}\frac{\partial lnp}{\partial r}}, \tag{14}$$

$$\sigma_{\rm SGI} = \sqrt{\frac{2\pi G(\rho_2 - \rho_1)^2}{(\rho_2 + \rho_1)}}. \tag{15}$$

The RT and SGI instabilities result in very similar configurations at density snapshots. However, they have their own characteristics, which allows us to differentiate between them. As self-gravity has no 'preferred' direction, it is destabilizing across all density interfaces, while an interface is RT-unstable only if the heavy fluid is on top of the light fluid. It has also been confirmed that RT instability is characterized by dense spikes penetrating the tenuous fluid, whereas the SGI develops with tenuous spikes streaming into the denser fluid.

We find that SGI instability seems to dominate over RT instability and produces the inhomogeneities. In particular, we checked that the growth rates of RT are having imaginary values, as computed at radii between 20 and 25 $r_{\rm g}$, around the mixing boundary.

Finally, we investigated the formation of transonic shocks in the collapsars. In Figure 5, we present radial profiles of Mach number at some specific time snapshots for models with $S = 2$ and $a_0 = 0.5$. The left panel shows the profiles in the self-gravitating case, while the plot in the right panel shows those of the self-gravitating magnetized case (we introduced a weak vertical magnetic field in the initial condition). For the sake of more visibility, we provide zoomed-in inset panels representing the inner regions. We observe the sonic front expansion and also some transient shock formation during the collapse. At early times, the small transonic shocks appear around 100 $r_{\rm g}$, and they present a moderate density contrast (pre-shock to post-shock density ratio $R = \rho_1/\rho_2 \sim 10$). Such shocks also appear at later times. Their formation is enhanced by the self-gravity effects. We find that the magnetic field does not make any significant difference in the shock expansion timescales, but it affects the strength of the shock, consistently with previous studies (Komissarov, 1999).

4 CONCLUSIONS

In this work, we show numerical models of the collapsing stellar core where we account for the dynamical evolution of central black hole mass and its spin. The related coefficients of the Kerr space-time metric are evolved accordingly, at every time step. In addition, we calculate the self-gravity of the stellar envelope, and we add the relevant perturbative terms to the dynamical evolution of the black hole spin parameter.

The last modification of the model turned out to have an impact on the global evolution of the collapsing star and produce dramatic fluctuations in the accretion rate at the initial

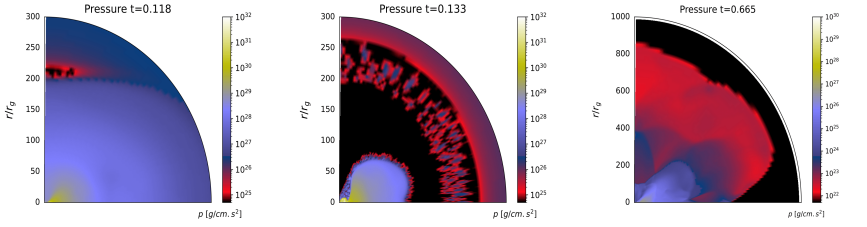

Figure 3. **Left:** Pressure profile for the model with rotation parameter S=2 and initial black hole spin $A_0 = 0.5$, taken at time t=0.118 s., at which largest accretion rate fluctuations appear. **Middle:** Pressure profile at time t=0.133, for the same model as in the left plot. Strong inhomogeneity regions are visible. **Right:** Pressure profile at a later time of the simulation for the same model as in the left and middle plots. Inhomogeneities are the same, and at this time, accretion rate fluctuations are smoothed as well. The map is zoomed out to a larger radius.

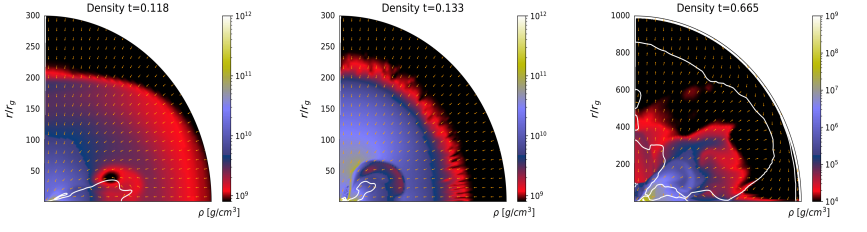

Figure 4. **Left:** Density profile at t=0.118, for the same model as above. **Middle:** Density profile at t=0.133, for the same model as above. **Right:** Density profile at late time, t=0.665, for the same model as above.

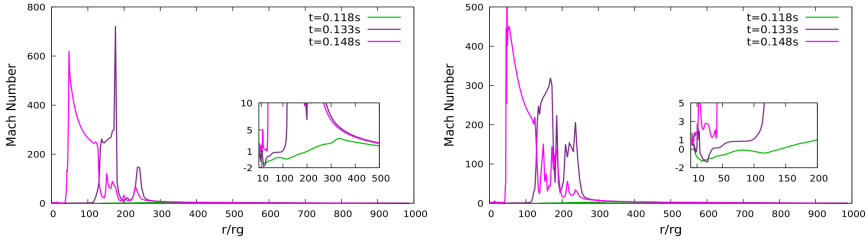

Figure 5. **Left:** Mach number profile at three different times, t=0.118, t=0.133, and t=0.148 s, for the model with $S = 2.0$. **Right:** Mach number profile at three different times for the same model with a magnetic field.

phase of collapse. More importantly, it also plays a crucial role in the development of the SGI interfacial instability in its specific regions. We identified inhomogeneities in density and pressure distributions which arise due to self-gravity, and we concluded that the SGI instability dominates over the RT, as its growth rate is positive in the regions of mixing boundaries.

ACKNOWLEDGEMENTS

The present work was supported by the grant DEC-2019/35/B/ST9/04000 from Polish National Science Center. We made use of computational resources of the PL-Grid infrastructure under grant pglgrb6 and Warsaw University ICM. D. Ł. K. was supported by the Polish National Science Center Dec-2019/35/O/ST9/04054, and N. Sh. D. was supported by Iran National Science Foundation (INSF) under project number No.4013178 and also acknowledges the Ferdowsi University of Mashhad (FUM), Iran, and the FUM Sci-HPC center. Prof. Shahram Abbassi also deserves gratitude for his accompaniment to N.Sh.D. in this project. A.J. acknowledges the Czech-Polish mobility program (MŠMT 8J20PL037 and PPN/BCZ/2019/1/00069).

REFERENCES

Gammie, C. F., McKinney, J. C. and Tóth, G. (2003), HARM: A Numerical Scheme for General Relativistic Magnetohydrodynamics, *Astrophysical Journal*, **589**(1), pp. 444–457, arXiv: astro-ph/0301509.

Hunter Jr, J. H., Whitaker, R. W. and Lovelace, R. V. (1997), Kelvin-helmholtz and thermal-dynamic instabilities with self-gravity: a new gravitational interface instability, *The Astrophysical Journal*, **482**(2), p. 852.

Janiuk, A., Shahamat Dehsorkh, N. and Król, D. Ł. (2023), Self-gravitating collapsing star and black hole spin-up in long gamma ray bursts, *Astronomy & Astrophysics*, **677**, A19, arXiv: 2304.01342.

Janiuk, A., Sukova, P. and Palit, I. (2018), Accretion in a Dynamical Spacetime and the Spinning Up of the Black Hole in the Gamma-Ray Burst Central Engine, *Astrophysical Journal*, **868**(1), 68, arXiv: 1810.05261.

Kifonidis, K., Plewa, T., Janka, H.-T. and Müller, E. (2003), Non-spherical core collapse supernovae-i. neutrino-driven convection, rayleigh-taylor instabilities, and the formation and propagation of metal clumps, *Astronomy & Astrophysics*, **408**(2), pp. 621–649.

Komissarov, S. S. (1999), Numerical simulations of relativistic magnetized jets, *MNRAS*, **308**(4), pp. 1069–1076.

Król, D. Ł. and Janiuk, A. (2021), Accretion-induced Black Hole Spin-up Revised by Numerical General Relativistic MHD, *Astrophysical Journal*, **912**(2), 132, arXiv: 2104.00741.